

Deep Stacked Stochastic Configuration Networks for Non-Stationary Data Streams

Mahardhika Pratama^a, Dianhui Wang^{b,c,*}

^a*School of Computer Science and Engineering, Nanyang Technological University, Singapore, 639798, Singapore*

^b*Department of Computer Science and Information Technology La Trobe University, Melbourne, VIC 3086, Australia*

^c*The State Key Laboratory of Synthetical Automation for Process Industries, Northeastern University, Shenyang, Liaoning Province 110819, China*

Abstract

The concept of stochastic configuration networks (SCNs) offers a solid framework for fast implementation of feedforward neural networks through randomized learning. Unlike conventional randomized approaches, SCNs provide an avenue to select appropriate scope of random parameters to ensure the universal approximation property. In this paper, a deep version of stochastic configuration networks, namely deep stacked stochastic configuration network (DSSCN), is proposed for modeling non-stationary data streams. As an extension of evolving stochastic configuration networks (eSCNs), this work contributes a way to grow and shrink the structure of deep stochastic configuration networks autonomously from data streams. The performance of DSSCN is evaluated by six benchmark datasets. Simulation results, compared with prominent data stream algorithms, show that the proposed method is capable of achieving comparable accuracy and evolving compact and parsimonious deep stacked network architecture.

Keywords: stochastic configuration networks, deep learning, non-stationary data streams

1. Introduction

The age of big data has led to urgent demand to fast data analytics having low complexity while producing an acceptable level of accuracy. The development of Internet of Things (IoT) has resulted in the ease of data collection and makes possible for continuous recording of data samples. That is, data are continuously sampled at a fast pace and creates a lifelong learning environment. In

*Corresponding author

Email addresses: mpratama@ntu.edu.sg (Mahardhika Pratama), dh.wang@latrobe.edu.au (Dianhui Wang)

other words, the problem size is unknown and possibly unbounded. This situation refers to the problem of data streams which must be handled in the online mode and in the sample-wise manner. The problem of data stream requires innovation of current data analytic methods [3, 14] since the vast majority of approaches adopt a batched learning scheme which assumes a fixed dataset and calls for a retraining phase whenever new knowledge is observed. Ideally, data mining methods should be capable of transforming fast information flow into useful reference in the one-pass training fashion to guarantee its scalability in the dynamic and lifelong learning environments.

Randomized approaches provide a plausible solution in the data-rich applications because it offers great simplification in the learning process [19, 32]. Although issue of randomized approaches in neural networks have received attention in the late 80's and early 90's, the benefit of such approaches becomes more evident in recent days with the emergence of deep neural networks (DNNs) involving a large number of network parameters where training all of those parameters incur considerable computational cost and prohibitive memory demand. The randomized approach relieve design steps of DNNs because it allows most DNN parameters but the output weights to be randomly generated from certain scopes and distributions. This mechanism speeds up algorithm's runtime which happens to be a key factor of scalability in the resource-constrained environments because the training process rely on no tuning of hidden nodes and is free from iterative training process. Random vector functional link network (RVFLNs) exemplify a successful integration of the randomized approaches in neural network [19, 21]. Specifically, RVFLN incorporates the randomized idea for construction of functional link neural network [20] and shares the universal approximation capability [11]. It is, however, reported that the universal approximation capability of RVFLN highly depends on the setting of the scope of random parameters and is hardly implemented in practise [11]. It is shown in [13] that the scope of random parameters plays vital role to retain the universal approximation property of RVFLN. The scope of random parameters should not be fixed and should be adaptively adjusted to adapt to different problem complexities [38].

Stochastic configuration networks (SCN) were recently proposed in [38] as an innovative and revolutionary solution to combat robustness issue in the randomized learning where improper setting of random parameters may fail the universal approximation property of the model. Unlike existing randomized approaches where the scope of random parameters is predefined and fixed, SCN applies a supervisory mechanism to assign the random parameters. It is also found that random parameters should have relevance on the training samples and should be data dependent. In [38], three algorithms to implement SCNs are proposed by tuning the output weights: direct, local least square and global least square. The SCN framework has been extended in [36] where the SCN theory is implemented in the context of deep neural networks (DNNs). Ensemble version of SCN was proposed in [35] which can be regarded as an advancement of DNNE [2]. It resolves the problem of large-scale pseudo-inverse computation using the block Jacobi and Gauss-Seidel approximation. A robust SCN was

designed in [37] for resolving robust data modeling problems using the kernel density estimation. Nonetheless, data stream remains an open issue for these existing SCNs because they work on a fixed dataset and learning environment is supposed to be unchanged during the course of training process.

Recent years have witnessed tremendous success of deep neural networks (DNNs) in numerous real-world applications. DNNs offer state-of-the-art performance for complex problems which are hard to be tackled by conventional machine learning methods [12]. Significant performance improvement can be achieved by inserting additional layers of neural networks and this characteristic is impossible to be attained by a shallow network architecture. Referring to stacked generalization principle [41, 42], deep network architecture brings advantage to generalization performance. The major success of DNNs depends very much on the architecture of DNNs which should be chosen at the right complexity. Too simple DNN architectures won't incur extra generalization power from those shallow networks, whereas too complex architecture will lead to the issue of overfitting [36]. The architecture of DNNs is usually determined from rigorous experimentation since not only the number of hidden nodes has to be selected but also the depth of DNNs has to be carefully assigned while the number of hidden nodes per layer may vary as well. Since the structure of DNNs is blindly selected, the structural complexity of DNNs may go beyond what is necessary. Because DNNs impose a large number of network parameters to adjust, training process of DNNs is slow and committed in the iterative manner. This problem can be addressed by performing a unsupervised learning process for parameter initialization but such solution is not compatible for online scenario. To arrive at convergence, DNNs incurs high sample consumption unless the overfitting problem may occur.

In this paper, we propose a novel version of deepSCNs termed deep stacked stochastic configuration networks (DSSCNs). DSSCN presents a highly scalable and deep solution for data stream since it works fully in the one-pass learning fashion where every data chunk is seen once and directly discarded afterward. It demonstrates an open structure principle where not only hidden nodes are automatically evolved and pruned from data streams but also hidden layers of DSSCN are self-organized. In other words, the selection of DSSCN's depth is fully data-driven while being able to reduce by pruning inconsequential hidden layers [30]. Our algorithm is capable of initiating its learning process from scratch with no initial structure. That is, hidden node and hidden layer can be incrementally added from data streams subject to the rule growing scenario and the drift detection method. DSSCN is built upon the stacked generalization principle [41, 48]. That is, the output of one learner is fed as an input to the next learner while each layer is given with the same input representation plus a random projection of the predictive output of the preceding layer. A drift detection scenario controls the depth of the DSSCN where a new layer can be added when a drift is identified. DSSCN implements complexity reduction mechanisms in terms of online feature weighting mechanism and hidden layer pruning scenario. DSSCN is underpinned by evolving stochastic configuration network (eSCN) which generalizes evolving random vector functional

link network (eRVFLN) [46]. eSCN realizes the learning pillars of SCN where assignment of random parameters is committed with inequality constraint and scope of random parameters is set to be fully adaptive. eSCN inherits characteristics of eRVFLN where both parameter learning and structural learning scenarios are fully automated. Novelty of DSSCN is outlined as follows:

1. Drift Detection Scenario: the evolving structure of DSSCN is governed by a drift detection scenario which identifies dynamic characteristics of data streams. A new layer is incorporated by constructing a new hidden layer if a drift is signalled. Drift detection scenario has been widely implemented in realm of ensemble learning where it controls when a new ensemble member is added [30]. Nevertheless, recent investigation in [42] has concluded that the increase of network depth make significant difference in generalization power. It is theoretically shown that a two layer neural network cannot solve a task that can be addressed by a three layer neural network unless it has an infinite number of hidden nodes. Our work aims to investigate the use of the drift detection scenario to signal when to incrementally augment the depth of neural networks. The drift detection scenario is devised from the Hoeffding’s bound theory which categorizes data streams into three conditions: drift, warning and normal[10]. The idea of Hoeffding’s bound allows the choice of conflict thresholds to be determined automatically with sufficient statistical guarantee.
2. Evolving Stochastic Configuration Networks: evolving stochastic configuration networks (eSCNs) is crafted in this paper where it is derived from evolving random vector functional link networks (eRVFLNs)[46]. Unlike its predecessor, eSCNs adopt the SCNs theory where inequality constraint is deployed when initializing the random parameters [38]. The concept of SCNs allows adaptive scope allocation where the scope of random parameters are not fixed to a specific range rather are dynamically selected. Furthermore, eSCNs characterize a fully evolving structure where hidden nodes can be automatically generated from scratch with no tuning of hidden nodes. The network output is inferred using the interval type-2 fuzzy system concept where interval type-2 multivariate Gaussian function with uncertain centroids. By extension, another innovation is seen in the one-pass learning scenario of eSCNs compared to the batch working principle in[38], where data streams are learned chunk by chunk in the one-pass fashion.
3. Deep Stacked Neural Networks Architecture: DSSCN is actualized under a deep stacked neural networks structure where every layer is formed by a base-learner, eSCNs. The stacked neural network architecture is built upon the stacked generalization principle where the training samples of every layer are drawn from original training samples mixed with random shifts. Random shift is induced by random projection of predictive outcomes of preceding layer/learner. This idea is inspired by the deep TSK fuzzy learners in [48]. Here, we go one step further by introducing the self-organizing concept of DNN’s structure encompassing hidden nodes,

input features and depth of the networks.

4. Online learner Merging Scenario: DSSCN is equipped with a complexity reduction method using the learner merging strategy. The learner merging strategy analyzes the output of base learners and two base learners sharing high similarity are coalesced to alleviate complexity and risk of overfitting. The learner merging scenario is enabled in the DSSCN because it features a stacked architecture where the output of base learner is utilized as a shifting factor to the next base learner. In other words, each layer is supposed to output the same predicted variables.
5. Online Feature Weighting Scenario: DSSCN features the online feature weighting mechanism based on the notion of feature redundancy [28]. This mechanism deploys feature weights for every layer where features exhibiting high mutual information is assigned with low weights. Moreover, feature weights are not fixed and dynamically tuned as the redundancy level of input attributes.

Learning performance of DSSCN has been evaluated by exploiting five popular streaming data sets and one real-world application from our own project, RFID based Indoor localization. It is also compared with six data stream algorithms, pClass [24], eT2Class [29], pEnsemble [30], Learn++CDS [8], Learn++NSE [9] and its shallow version, eSCN. DSSCN demonstrates improvement of classification rates over its counterparts while imposing comparable computational power and network parameters. Compared to the shallow version, 2% to 5% improvement of predictive accuracy can be achieved with extra computation and storage complexity. The remainder of this paper is organized as follows: Section 2 elaborates the learning mechanism of eSCN; Section 3 discusses the working principle of DSSCN consisting of the stacked network structure, the drift detection scenario, the online learner merging method, and the online feature weighting mechanism; Section 4 describes experimental study; some concluding remarks are drawn in the last section of this paper.

2. Evolving Stochastic Configuration Networks

eSCNs utilize a combination of the multivariate Gaussian basis function and the up-to second order Chebyshev functional expansion block which enhances the original input pattern into a set of linearly independent functions of the entire input attributes [22]. The output of Chebyshev functional expansion block is weighted by the activation degree of each hidden node generated by the multivariate Gaussian basis function and the output weights. In other words, the output layer consists of linear combinations of input features and output weights resulting in the second order polynomial series. This notion is inspired by the functional-link neural network structure (FLNN) where it features the so-called enhancement node combining two components: a direct connection of the input layer to the output layer and a functional expansion block performing

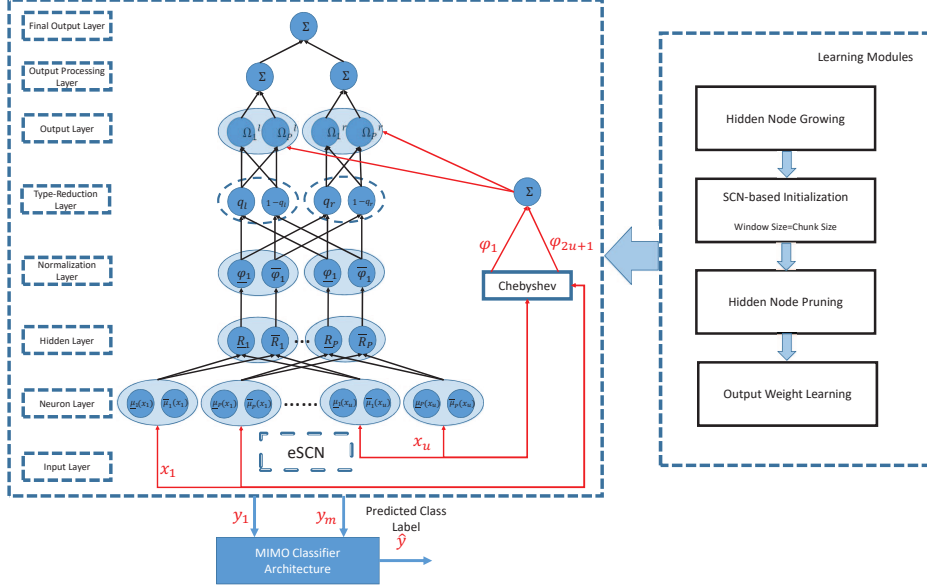


Figure 1: Learning Architecture of eSCNs

a non-linear transformation of original input space to a higher dimensional space [20]. The multivariate Gaussian basis function is developed by a non-diagonal covariance matrix featuring inter-correlation between two input variables [23]. DSSCN works fully in the one-pass learning fashion where, at any given time, only one sample is seen whereas other data are discarded once learned.

Suppose that a tuple (X_t, T_t) streams at time-instant t th where $X_t \in \mathfrak{R}^n$ denotes an input feature of interest and $T_t \in \mathfrak{R}^m$ stands for the target variable, the end output of DSSCN can be expressed as follows:

$$y_o = \sum_{i=1}^R \tilde{G}_i(A_i \cdot X_t + B_t)\beta_i, \quad (1)$$

where $A_i \in \mathfrak{R}^n$ is the input weight vector of the i -th hidden node obtained from the online feature weighting mechanism in Section 4.1 and \tilde{G} is the activation function of eSCN defined as the interval-valued multivariate Gaussian function. B_t is the network bias set as zero for simplicity, while R is the number of hidden nodes, n is the number of input dimension and m is the number of output dimension. $\beta_i = x_e W_i$ where $x_e \in \mathfrak{R}^{1 \times (2n+1)}$ is the extended input vector produced by the functional expansion block of second order Chebyshev function while $W_i \in \mathfrak{R}^{(2n+1) \times 1}$ is the output connective weight vector. The functional-link strategy in the output layer expands the degree of freedom (DOF) supposed to improve approximation power of the output node. Note that the original SCN is developed using the zero-order output node where it embraces only one single component weight $W_i \in \mathfrak{R}^1$. The extended input vector, x_e , is crafted from

a nonlinear mapping of the Chebyshev polynomial expansion up to the second order written as follows:

$$T_{n+1}(x_j) = 2x_jT_n(x_j) - T_{n-1}(x_j), \quad (2)$$

where $T_0(x_j) = 1, T_1(x_j) = x_j, T_2(x_j) = 2x_j^2 - 1$. Suppose that the number of input dimension is two, the extended input vector, x_e , is set as:

$$x_e = [1, T_1(x_1), T_2(x_1), T_1(x_2), T_2(x_2)] = [1, x_1, 2x_1^2 - 1, x_2, 2x_2^2 - 1]. \quad (3)$$

The intercept, 1, is inserted in the extended input vector and is meant to prevent the untypical gradient problem [27]. In addition, it increases flexibility allowing the extended input vector to go beyond the origin if all input attributes possess zero values. The functional expansion block is performed by the Chebyshev polynomial here rather than other functional-link types such as trigonometric or polynomial functions since it scatters less number of parameters than trigonometric function and offers better mapping capability than other polynomial functions of the same order.

A crisp activation degree is produced by performing the type reduction mechanism using the q type-reduction mechanism of the interval-valued activation degree \tilde{G}_i [16] as follows:

$$\tilde{G}_i = (1 - q)\overline{G}_i + q\underline{G}_i, \quad (4)$$

where $q \in \mathfrak{R}^{1 \times m}$ is a design coefficient which adjusts the influence of upper and lower activation degrees. $\underline{G}_i, \overline{G}_i$ denote the lower and upper activation functions satisfying the condition of $\overline{G}_i > \underline{G}_i$. The upper and lower activation functions $\underline{G}_i, \overline{G}_i$ are resulted from the multivariate Gaussian basis function with uncertain means characterized by the non-diagonal covariance matrix [29]. This strategy adopts the notion of interval type-2 fuzzy system presenting the footprint of uncertainty [1] which aims to capture possible inaccuracy, imprecision and uncertainty of data streams due to noisy measurement, noisy data, operator's error, etc. It is worth mentioning that the vast majority of interval type-2 fuzzy systems in the literature is essentially akin to the interval-valued fuzzy system where only a single interval is incorporated. The interval type-2 fuzzy system generalizes the interval-valued fuzzy system where it includes the multi-interval case [33]. The q type reduction method is applied here because it characterizes a faster operation to transform the interval-valued activation degrees to its crisp form than the prominent Karnik-Mendel (KM) method usually involving the iterative process to obtain the right-most and left-most points. The interval-valued multivariate Gaussian basis function, \tilde{G}_i , is expressed as follows:

$$\tilde{G}_i = \exp(-(X - \tilde{C}_i)\Sigma_i^{-1}(X - \tilde{C}_i)^T), \quad \tilde{G}_i = [\underline{G}_i, \overline{G}_i], \quad (5)$$

where $\tilde{C}_i = [\underline{C}_i, \overline{C}_i]$ denotes the interval-valued centroid and $\underline{C}_i < \overline{C}_i$. Σ_i^{-1} labels the inverse non-diagonal covariance matrix whose elements describe interrelation between two input features. The interval-valued multivariate Gaussian

basis function generates the non-axis-parallel ellipsoidal cluster in the product space which has an aptitude to rotate in any direction. Such ellipsoidal cluster offers flexibility in capturing irregular data distribution which does not span in the main axes [23]. This property possesses low fuzzy rule demand which compensates possible increase of network parameters as a result of the non-diagonal covariance matrix [15].

The upper and lower activation degree (3) can be derived further using the principle of interval type-2 fuzzy system where the expression of upper and lower activation functions $\underline{G}_i, \overline{G}_i$ can be obtained. This step, however, calls for a transformation mechanism to be carried to adapt to the working formula of interval type-2 Gaussian function with uncertain means. The transformation strategy finds a one-dimensional representation of high-dimensional Gaussian function where the center-to-cutting point distance of the non-axis-parallel ellipsoidal cluster is analyzed. This transformation strategy offers a fast transformation mechanism because no eigenvalues and eigenvectors have to be calculated in every observation but it is rather inaccurate to represent an ellipsoidal cluster with around 45 degrees rotation. Since the centroid of the ellipsoidal cluster C_i remains the same when projected to one dimensional space, the focus of transformation strategy is to elicit the radii of high-dimensional multivariate Gaussian activation σ_i in the low dimension as follows:

$$\sigma_i = \frac{\tilde{r}_i}{\sqrt{\tilde{\Sigma}_{i,i}}} = \tilde{r}_i \sqrt{\Sigma_{i,i}^{-1}}, \quad (6)$$

where $\tilde{r}_i = \frac{r_i + \bar{r}_i}{2}$ is the Mahalanobis distance of the i th rule to an incoming samples and $\Sigma_{i,i}^{-1}$ is the diagonal elements of inverse covariance matrix. The same centroid can be applied in the one-dimensional space without any amendment. Once the low dimensional representation of multivariate Gaussian function is extracted, the same concept of interval type-2 fuzzy system can be adopted to quantify the interval-valued activation degrees as follows:

$$\bar{\mu}_{i,j} = \begin{cases} N(\underline{c}_{i,j}, \sigma_{i,j}; x_j), & x_j < \underline{c}_{i,j} \\ 1 & \underline{c}_{i,j} \leq x_j \leq \bar{c}_{i,j} \\ N(\bar{c}_{i,j}, \sigma_{i,j}; x_j) & x_j > \bar{c}_{i,j}, \end{cases} \quad (7)$$

$$\underline{\mu}_{i,j} = \begin{cases} N(\bar{c}_{i,j}, \sigma_{i,j}; x_j) & x_j \leq \frac{\bar{c}_{i,j} + \underline{c}_{i,j}}{2} \\ N(\underline{c}_{i,j}, \sigma_{i,j}; x_j) & x_j > \frac{\bar{c}_{i,j} + \underline{c}_{i,j}}{2}, \end{cases} \quad (8)$$

Once the activation degree per input attribute is elicited using (5), (6), it is combined using the product t-norm operator to induce the upper and lower activation degrees $\underline{G}_i, \overline{G}_i$ as follows

$$\underline{G}_i = \prod_{j=1}^n \underline{\mu}_{i,j}, \overline{G}_i = \prod_{j=1}^n \bar{\mu}_{i,j}. \quad (9)$$

The use of the product t-norm operator in (7) opens possibility to apply the gradient-based learning approach compared to the min t-norm operator. Nevertheless, the flaw of this t-norm operator is apparent when dealing with a high input dimension because interval-valued activation degree decreases as the input variables increase. For simplicity, the final output expression of DSSCN (1) can be also expressed in one compact form as follows:

$$y_o = \frac{(1 - q_0) \sum_{i=1}^R \underline{G}_i \beta_i + q_0 \sum_{i=1}^R \overline{G}_i \beta_i}{\sum_{i=1}^R (\overline{G}_i + \underline{G}_i)}, \quad (10)$$

where q_o is the design coefficient of the o -th target class performing the type reduction mechanism. The MIMO architecture is implemented here to infer the final predicted class label of eSCN where each rule comprises multiple output weights per each class attribute. That is, the MIMO architecture is supposed to resolve the class overlapping issue because it takes into account each class specifically by deploying different sets of output weights per class [3]. This approach is more robust in handling the class overlapping problem than the popular one versus rest method because it retains the original class structure. The final predicted class of eSCN is written as follows:

$$y = \max_{1 \leq o \leq m} (y_o). \quad (11)$$

The MIMO structure starts from encoding of true class label to the vector form where a component is assigned to “1”. Suppose that if the true class label is 2 and the output dimension is 3, the true class label vector is expressed as $T = [0, 1, 0]$. This scenario differs from the direct regression of class label which does not cope with steep class changes. This drawback is caused by the nature of regression-based classification scheme where there exists a smooth transition when regressing to the true class label. Figure 1 exhibits the network architecture of eSCN.

3. Deep Stacked Stochastic Configuration Networks

Deep stacked architecture of DSSCNs is inspired by the work of [48] featuring a series of base building units working in tandem. That is, each base building unit is structured by eSCNs which receives the original input attributes added by the random shift. The novelty of DSSCNs lies in its autonomous working principle where the deep stacked architecture can be automatically deepened and shallowed. The random shift is induced by the random projection of the predictive output of the preceding layer which aims to follow the stacked generalization principle. The deep stacked architecture allows continuous refinement of predictive output through multiple nonlinear mapping of base building units. The architecture of deep stacked structure is depicted in Figure 2. DSSCN works in chunk by chunk basis where each chunk containing N pairs of tuples $(X_t, T_t)_{t=1, \dots, N}$ streams overtime and the total number of chunks is unknown.

It is worth mentioning that DSSCN adopts a strictly single-pass learning process where each data chunk is discarded once learned. In realm of deep stacked network architecture, it is almost impossible to adopt the sample by sample update since the hierarchical structure of deep stacked network relies on the output of the preceding layer. That is, the output of the preceding layer must feed meaningful information for the next layer to lessen the predictive error toward zero.

The first building block or layer is injected with the original data chunk $X_1 = (X_t)_{t=1, \dots, N}$ and in turn generates the predictive outputs $Y_1 = (Y_t)_{t=1, \dots, N}$. The stacked generalization principle is implemented in the next layer where the output of the first building unit is connected to the second layer and mixed with the random projection matrix. The input of the second building block is formulated as follows:

$$X_2 = X + \alpha Y_1 Z_1, \quad (12)$$

where α is a random projection constant and $Z_1 \in \mathbb{R}^{m \times n}$ is the random projection matrix randomly generated in the range of $[0,1]$. It is observed in (10) that the right term $\alpha Y_1 Z_1$ is treated as the random shift of the original input attributes which aims to capture a high level abstraction of the original input features. The stacking strategy continues up to the last building block whose input is determined as $X_D = X + \alpha Y_{D-1} Z_{D-1}$ where D stands for the depth of DSSCN. It is worth noting that DSSCN demonstrates the fully elastic deep network structure where a new building unit can be inserted on top of the current hidden layer when the existing structure does not suffice to a given problem. All layers or building blocks are stacked and work in tandem where each layer except the bottom layer produces random shifts of original input pattern to be passed to the next layer.

It is evident that the notion of random shifts in each layer of DSSCN improves linear separability of given classification problem because it paves a way to move apart the manifolds of original problem in a stacked manner [48]. This structure is also perceived as a sort of hierarchical structure but it differs from the conventional hierarchical deep neural network which generally loses transparency of intermediate features because it can no longer be associated with physical semantics of original input features [47]. It is also worth mentioning that DSSCN is equipped by the online feature selection mechanism coupled in every building unit. This mechanism selects relevant input attributes for every layer which enhances generalization power.

4. Learning Scheme of DSSCN

This section elaborates the learning policy of DSSCN including the fundamental working principle of eSCN as the base building block of DSSCN. Algorithm 1 displays an overview of DSSCN learning algorithm. DSSCN working

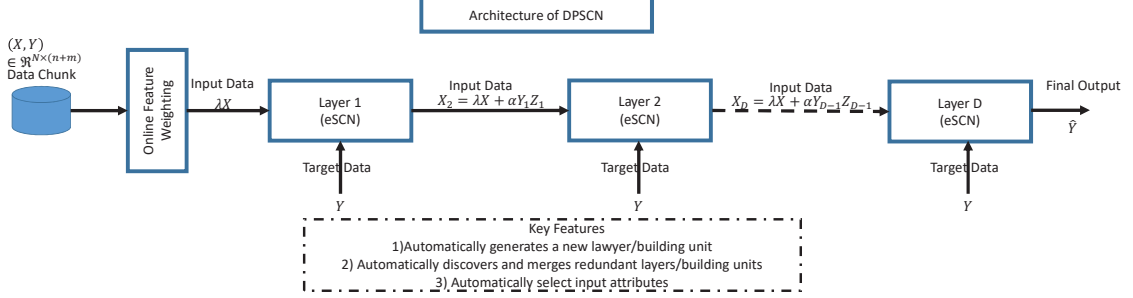


Figure 2: Architecture of DSSCN Model

Table 1: Pseudocode of DSSCN learning policy

<p>Input: Data Chunk $(X, Y) \in \mathbb{R}^{N \times (n+m)}$, the layer merging threshold δ, the time-constants of the Hoeffding's based drift detection method T_D, T_W, the random projection constant α</p> <p>Output: Predicted Class labels $\hat{Y} \in \mathbb{R}^{N \times (n+m)}$, DSSCN structure with D depth or layers</p> <p>$f(layer_1(C \in \mathbb{R}^{R \times n}, \Sigma^{-1} \in \mathbb{R}^{R \times (n \times n)}, W \in \mathbb{R}^{R \times (2n+1) \times 1}), \dots, layer_D(C \in \mathbb{R}^{R \times n}, \Sigma^{-1} \in \mathbb{R}^{R \times (n \times n)}, W \in \mathbb{R}^{R \times (2n+1) \times 1}))$</p> <p>For $t = 1, \dots, N$ // loops over all samples in the data chunk</p> <p>For $j = 1, \dots, n$ // Section 4.1 Online Feature Weighting Mechanism</p> <p>For $q = 1, \dots, n$</p> <p>Calculate the similarity of two input features $\gamma(x_j, x_q), j \neq q$</p> <p>Form the input weighth vector $\lambda \in \mathbb{R}^{1 \times n}$</p> <p>END FOR</p> <p>END FOR</p> <p>IF depth is zero</p> <p>Create the first layer or base building unit $D = 1$ // execute Section 4.4 eSCN learning policy</p> <p>ELSE</p> <p>For $d = 1, \dots, D$ // loops over all layers and execute Section 3.2 deep stacked network structure</p> <p>IF $d = 1$</p> <p>$X_1 = X$</p> <p>Elicit the output of each layer // The forward-pass mechanism of eSCN (Section 3.1)</p> <p>ELSE IF</p> <p>$X_d = X + \alpha Y_{d-1} Z_{d-1}$</p> <p>Elicit the output of each layer // The forward-pass mechanism of eSCN (Section 3.1)</p> <p>END IF</p> <p>END FOR</p> <p>END IF</p> <p>FOR $i = 1, \dots, D$ // Calculate pairwise similarity - Section 4.2 Network Layer Merging Mechanism</p> <p>FOR $k = 1, \dots, D, i \neq k$</p> <p>Calculate similarity of two layers $\gamma(y_i, y_k), i \neq k$</p> <p>IF $\gamma(y_i, y_k) \leq \delta$</p> <p>Merge the layer i and k</p> <p>END IF</p> <p>END FOR</p> <p>END FOR</p> <p>Undertakes the drift detection method // Section 4.3 Network Layer Growing Mechanism</p> <p>IF Drift</p> <p>Introduces a new base building unit/layer // Section 4.4 eSCN learning policy</p> <p>ELSE IF Warning</p> <p>Do nothing and prepare for a possible drift in the next observation</p> <p>ELSE IF Stable</p> <p>Update the top hidden layer</p> <p>END IF</p> <p>END FOR</p>
--

procedure starts from the online feature weighting principle adopting the concept of mutual information. An input feature showing significant redundancy is ruled out from the training process by setting its corresponding input weight to small values. This mechanism does not compress input dimension but actively selects the best input subset for every training observation by means of dynamic weighting strategy of input features minimizing the influence of poor features. Henceforth, the training procedure of each layer is triggered and the first layer of DSSCN receives the original input features. The output of the first base building unit is combined with random projection matrix to induce the so-called random shift. The shifting factor is applied to the original input attributes feeding the next base building unit. This process proceeds up to the deepest layer.

DSSCN is fitted with the layer merging mechanism benefiting from the notion of mutual information. This concept unveils two base building units possessing strong mutual information. Such base building blocks do not offer diverse information to rectify learning performance and can be fused into one to relieve the computational complexity. The last step concerns with the drift detection scenario which evolves the structure of DSSCNs. This mechanism controls the depth of DSSCNs where an extra building unit is added and the structure of DSSCNs is deepened provided that a concept change is observed. This scenario is built upon the concept of Hoeffding’s bound where the drift detection mechanism is fully automated and free of user-defined parameters. The conflict level is determined from a statistically sound method of the Hoeffding’s bound. The novelty of DSSCNs is present in its fully elastic structure. That is, the hidden node, network layer and input variables are automatically generated and pruned on the fly to produce proper complexity of the given problems.

4.1. Online Feature Weighting Mechanism

DSSCN is equipped by the online feature weighting mechanism which allocates input weights as the importance of input attributes. This mechanism is meant to minimize the influence of poor features which often undermines generalization power. Note that the use of online feature weighting mechanism underpins a compact and parsimonious structure because it rules out inconsequential features from the distance calculation [28]. In realm of evolving data streams, the feature weighting mechanism has been studied as an alternative of the input pruning method and is claimed to induce the soft-dimensionality reduction [25]. It offers more stable feature selection mechanism than its counterpart, the hard-dimensionality reduction approach, because it adapts to dynamic of given problems - some features play vital role in different time periods, thus pruning such features causes information loss. There exist a number of works in this problem domain where most of which are constructed under the Fisher separability criterion (FSC) method [24]. The generalized online feature selection (GOFs) method in [39] differs from these works where it adopts the crisp weighting concept (0 or 1). All of these approaches analyze the feature contributions without considering the redundancy of input features. The mutual information of input features are supposed to supply reliable information

of input features because it is less sensitive to changing system dynamics than the contribution-based feature selection mechanism.

The online feature weighting mechanism of DSSCN is inspired by the work in [28] where the maximal information compression index (MICI) method [17] is made use to calculate the feature similarity. The underlying idea is to assign low weight to a feature with strong mutual information. The MICI method presents an extension of Pearson correlation index where it is robust against translation and rotation of data streams. This method can be directly used for the feature weighting mechanism without transformation because an input feature has maximum correlation when the MICI method returns 0 values. Suppose that the linear dependency of two input variables, x_1 , x_2 are to be measured, the MICI is formulated as follows:

$$\gamma(x_1, x_2) = \frac{1}{2}(var(x_1) + var(x_2) - \sqrt{(var(x_1) + var(x_2))^2 - 4var(x_1)var(x_2)(1 - \rho(x_1, x_2)^2)}), \quad (13)$$

where $\rho(x_1, x_2) = \frac{cov(x_1, x_2)}{\sqrt{var(x_1)var(x_2)}}$ is the Pearson correlation index. $var(x_1), var(x_2)$ denote the variance of two features which can be enumerated on the fly. The MICI method works by estimating maximum information loss when the input dimension is compressed by ignoring one of the input features. After the MICI is obtained, the similarity score of input attributes is inspected because correlation of input features has to be analyzed for the rest $n - 1$ features ($\gamma(x_1, x_2), \dots, \gamma(x_1, x_{n-1})$). The similarity score is defined as the average of mutual information for all input attributes as follows:

$$Score_j = \text{mean}(\gamma(x_j, x_l)), l \neq j. \quad (14)$$

$j=l=1, \dots, n$

A normalization is required because it is expected that feature contribution drops in the high-dimensional input attributes. Input weights, λ_j , are normalized in respect to the maximal similarity score as follows:

$$\lambda_j = \frac{Score_j}{\max_{j=1, \dots, n}(Score_j)}. \quad (15)$$

It is worth noting that the input weights function as the connective weights of the first layer to the hidden layer of eSCN. Since each building unit receives the same input information added with different random shifts, the input weighting mechanism is committed in the centralistic manner. In other words, the input weights are spread across each building unit. This is made possible because every layer is injected with the same input representation and the only difference merely lies in the random shift factors which vary across different layers. This approach follows a similar input weighting strategy in [28] but here it is implemented under a deep network structure rather than a shallow one.

4.2. Hidden Layer Merging Mechanism

The notion of network layer merging mechanism is motivated by the fact that each base building unit should navigate to an improvement of learning performance. Two strongly correlated base building blocks can be merged into one thereby alleviating computational and memory burdens. In realm of deep learning literature, there exist several attempts for complexity reduction of DNN but most of which are built upon the concept of regularization where inconsequential layer is weighted by small regularization factors [31]. In [44], the concept of merging is utilized to reduce the complexity of DNN but this approach concerns on a merging process of hidden units in the same layer. Our approach differs from existing works where the focus of investigation is to combine base building units or hidden layers of DNNs.

The network layer merging mechanism examines the mutual information among base building units discovering two base building units with strong mutual information. This strategy is carried out using the MICI method as with the online feature weighting mechanism and the only difference from the online feature weighting mechanism exists in the variables of interest where the output of two base building units are evaluated as follows:

$$\gamma(y_i, y_k), i \neq k, \quad (16)$$

where y_i, y_k respectively denote the predictive output of i, k building units. Although the MICI method forms a linear correlation measure, it can be executed more fastly than the non-linear correlation measure such as the symmetrical uncertainty method by means of the entropy measure. The entropy measure often necessitates discretization of input samples or the Parzen density estimation method. Simplification is commonly applied in the entropy measure where the training data is assumed to follow normal distribution as shown in the differential entropy method. Because the maximum linear correlation is attained provided that $\gamma(y_i, y_k) = 0$, the layer merging condition is formulated as follows:

$$\gamma(y_i, y_k) \leq \delta, \quad (17)$$

where α stands for a user-defined threshold. The layer merging process is undertaken by getting rid of one of the two layers or in other words, the layer merging process shrinks the network structure. No hidden node transfer is necessary since one learner perfectly recovers another one. The layer merging mechanism enables hard complexity reduction where the base building unit is permanently forgotten since redundant layer won't be recalled again in the future. Unlike soft-complexity reduction [31, 45] where base building units are still retained in the memory, the hard complexity reduction attains great structure simplification by reducing the depth of network structure.

4.3. Hidden Layer Growing Mechanism

The selection of DSSCN network depth is fully automated from data streams in which this mechanism allows to find a right complexity of the given problem.

The network layer growing mechanism is governed by a drift detection mechanism which inserts a new base building unit if a concept change is identified in the data streams. This strategy is inspired by the fact that a new concept should be embraced by a new layer without forgetting of previously learned concept. It retains old knowledge in order for catastrophic forgetting of past knowledge which might be relevant again under the recurring drift situation to be avoided. Although the notion of drift detection mechanism is often integrated in the context of ensemble learning in which the size of ensemble expands if the drift is detected, this feature can be also implemented in realm of the deep stacked network since it is formed by a collection of local learners injected with different level of abstractions of the original data points. Note that although each layer of DSSCN is connected in series, each layer locally learns data streams with minor interaction with other layers.

DSSCN makes use of the Hoeffding’s bound drift detection mechanism classifying data stream category into three categories: normal, warning and drift [10]. That is, the normal condition indicates stable concept which can be handled by simply updating the current network structure. The update strategy applies only to the top base building unit because of the inter-related nature of deep stacked architecture where one base building unit is influenced by the output of preceding layer or base building unit. This strategy aims to induce different representations of the original training pattern where each hidden layer portrays different perspective of the overall data distribution. It differs from the ensemble configuration where one base building unit is decoupled from the rest of ensemble members and under this configuration the winning learner should be selected for the fine-tuning phase. The drift phase pinpoints an uncovered concept which calls for enrichment of existing structure by integrating a new layer. The warning phase is designed to cope with the gradual drift since it signals immature drifts requiring several training observations to be borne out as a concrete drift. No action is carried out in the warning phase except to prepare existing structure for a drift case in the future. It is worth noting that the gradual drift is more difficult to be tackled than the sudden drift because the drift can be confirmed at very late stage after the learning performance has been compromised. The non-weighted moving average version of the Hoeffding’s bound drift detection mechanism is implemented in DSSCN because it is more sensitive to the sudden drift than the weighted moving average version. The statistics of data streams can be enumerated without any weights as $\hat{X}_t = \sum_{i=1}^N \frac{x_i}{N}$.

The three conditions of data streams, namely normal, warning and drift are determined from the Hoeffding test applying two conflict levels: α_W (warning), α_D (drift) which correspond to the confidence level of the Hoeffding’s statistics as follows:

$$\varepsilon_\alpha = (b - a) \sqrt{\frac{(N - cut)}{2cut(N - cut)} \ln\left(\frac{1}{\alpha}\right)}, \quad (18)$$

where $[a, b]$ denotes the minimum and maximum of data streams and α is the

significance level level where $\alpha_W > \alpha_D$. *cut* denotes the cutting point which indicates the inflection point from one concept to another. Note that the significance level has a clear statistical interpretation because it also functions as the confidence level of Hoeffding’s bound $1 - \alpha$. The drift detection mechanism partitions a data chunk into three groups $Z_1 = [x_1, x_2, \dots, x_{cut}]$, $Z_2 = [x_{cut+1}, x_{cut+2}, \dots, x_N]$, $Z_3 = [x_1, x_2, \dots, x_N]$ where the cutting point corresponds to a switching point signifying a case of $\hat{Z}_1 + \varepsilon_{\hat{Z}_1} \geq \hat{Z}_3 + \varepsilon_{\hat{Z}_3}$. \hat{Z}_1, \hat{Z}_3 are statistics respectively calculated from two data groups Z_1, Z_3 . In other words, the cutting point refers to a case when a population mean increases. The drift detection procedure continues by forming the Hoeffding’s test which decides the status of data streams. The drift status is returned if the null hypothesis is rejected with the size of α_D , while the warning status makes use of α_W to reject the null hypothesis. The null hypothesis is defined as $H_0 : E(\hat{Z}_1) \leq E(\hat{Z}_2)$ while its alternative is formulated just as the opposite. The null hypothesis is rejected if $|\hat{Z}_1 - \hat{Z}_2| \geq \varepsilon$ where ε is found from (19) by applying the specific significance level α_W, α_D . The hypothesis test is meant to investigate the increase of population mean which hints the presence of concept drift. If the null condition is maintained, existing concept remains valid.

From Algorithm 1, it is seen that an extra layer is inserted if the drift status is substantiated by the drift detection mechanism. This mechanism aims to incorporate a new concept using a new layer while retaining previous knowledge in preceding layers. The warning phase does not perform any adaptation mechanism since it presents a waiting period whether the stable concept turns into the concept drift. Since the stable status confirms relevance of existing learners for current data streams, only an update is committed to the top building unit. This approach reflects the nature of deep network structure where each layer is interconnected in terms of random shift. We select to only adjust the top layer because it has the most adjacent relationship to the current training concept. Other layers are left untrained with the current data stream to generate different levels of feature representation - the key success of DNNs.

It is evident that the DNN concept is not feasible for small datasets. A shallow neural network is preferred for small datasets since it achieves a faster convergence due to less free parameters to learn than the DNNs. As more examples are observed, the performance of shallow neural networks is rather compromised and is able to be rectified by introducing extra layers in the neural network structure. In other words, the success of DNNs’s deployment is subject to sample’s availability. The significance level α plays vital role to arrive at the appropriate network architecture of DNNs since it controls the depth of neural network. It is not assigned a fixed value here rather constantly adjusted to adapt to current learning conditions where it grows proportionally as a factor of the number of data streams. That is, the confidence level is lowered to allow additional layers or building units to be integrated. The following setting is formulated to assign the confidence level:

$$\alpha_D = \min(1 - e^{-\frac{t}{T}}, \alpha_{min}^D), \alpha_W = \min(1 - e^{-\frac{t}{T}}, \alpha_{min}^W), \quad (19)$$

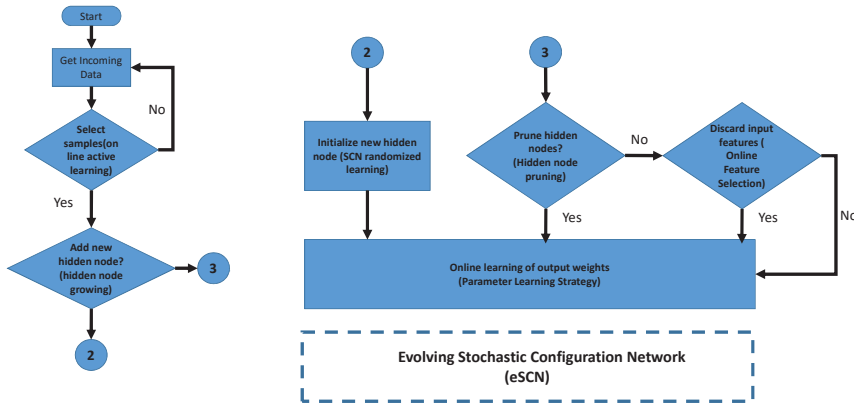


Figure 3: Evolving Stochastic Configuration of eSCN

where t denotes the number of data streams seen thus far. T is a time-constant which can be set as that of the number of time-stamp. If the number of time-stamp is unknown as practical scenarios, T can be assigned a particular value to produce moderate rise of exponential function. $\alpha_{min}^D, \alpha_{min}^W$ stand for the minimum significance level of drift and warning phases respectively fixed at 0.09 and 0.1. This setting is meant to set the confidence level to be above 90% which avoids loss of control for the increase of network depth. This considers the fact that the hidden layer growing strategy is built upon the drift detection scheme which risks on the loss of detection aptitude provided that the minimum confidence level is set too low. Referring to (12), it is assumed that the significance degree mimics the first-order system dynamic where it exponentially increases as the factor of time stamp. It is, however, limited to a certain point to avoid too small confidence level leading to be too greedy in generating new layers.

4.4. Learning Algorithms

This sub-section reviews the working principle of eSCN activated during the model update phase - the stable condition. eSCN features a fully open structure in which its hidden node can be automatically generated and pruned on the fly while following the randomized learning principle of stochastic configuration network (SCNs). eSCN is a derivation of eRVFLN [46] where the randomized learning foundation is constructed from the recent development of SCNs. Unlike its predecessor, two learning modules, online active learning and online feature selection, are switched off because the online feature selection is carried out in the centralistic mode based on the online feature weighting strategy putting forward the feature redundancy principle (Section 4.1). It is found that the use of online active learning scenario in each base building unit is not effective in reducing training samples and labelling cost since this approach is model-dependent and leads each base building unit to extract different data subsets -

impossible to be carried out under the deep stacked network configuration. It is supposed to work more efficiently in the centralistic configuration which sends same data samples for each building unit. eSCN learning scenario starts from scratch and the network structure can be self-constructed from data streams. The contribution of data streams are estimated by a generalized recursive density estimation principle [4]. The validity of fuzzy rules are monitored using the type-2 relative mutual information method and scans for inconsequential rules to be obviated for the sake of network simplicity. Figure 3 pictorially exhibits the working principle of eSCN. The learning algorithms of eSCN are detailed as follows:

- **Hidden Unit Growing Strategy:** The hidden node growing procedure of eSCN is akin to that of eRVFLN exploiting the concept of recursive density estimation [4]. It distinguishes itself from the original recursive density estimation method in the use of weighting factor which aims to address the large pair-wise distance problem after observing outliers or remote samples [40]. The underlying working principle of this approach is to calculate an accumulated distance of a sample with all other samples seen thus far without keeping all samples in the memory. Moreover, our approach is designed for a non-axis-parallel ellipsoidal cluster whereas the original version only covers the hyper-spherical cluster case. The advantage of this approach is relatively robust against outliers because it takes into account overall spatial proximity information of all samples. The hidden node growing criteria are formulated under two conditions. The first condition is set from the fact where a sample having high summarization power improves generalization potential of hidden nodes. A data sample with the highest density is added to be a new hidden node. The second condition is defined to expand the coverage of existing structure which captures non-stationary environments. This setting is realized by incorporating samples with the lowest density which indicates possible concept change. This condition leads to the necessity of a hidden node pruning scenario because such rule may not be supported by the next training samples. Nevertheless, this condition is prone to outlier, thus calling for the hidden node pruning scenario to obviate superfluous hidden nodes which do not play significant role during their lifespan. In addition, the rule replacement condition as known as "the condition B" in [5] is integrated which forms a condition for an incoming sample to replace the closest hidden node. This condition addresses the overlap among hidden nodes and is undertaken by checking the firing strength of the new hidden node candidate (9). The similarity threshold is determined from the chi-square distribution with 5% to 30% critical level.
- **Hidden Node Pruning Strategy:** The hidden node pruning role is warranted to attain a compact and parsimonious network structure where it is capable of detecting and pruning inactive hidden nodes. This learning module prevents overfitting situation which exists due to many clusters sitting adjacent to each other. eSCN benefits from the type-2 relative mu-

tual information method (T2RMI) which presents an extension of RMI method for the type-2 fuzzy system. This method analyzes relevance of hidden node in respect to the current data trend by quantifying correlation of hidden nodes and target classes. That is, superfluous hidden nodes are specified as those having little correlation with up-to-date target concept induced by changing data distributions or outliers mistakenly inserted as hidden nodes. In the original eT2RVFLN, the symmetrical uncertainty method is used to measure the correlation of input features and the correlation of hidden units to the target classes. The MICI method can be also exploited as an alternative. The symmetrical uncertainty method forms a nonlinear correlation measure where it is based on the information gain and entropy analysis. This method utilizes the differential entropy concept using the normal distribution assumption.

- **Parameter Learning Strategy:** all network parameters except the output weights are randomly initialized using the SCN concept while the output weights are updated on the fly using the fuzzily weighted generalized recursive least square (FWGRLS) method [26]. The FWGRLS method can be seen as a generalization of FWRLS method [4] where it distinguishes itself from its predecessor in the use of weight decay term in the cost function of RLS method. This leads to completely different tuning formulas but under some simplifications the final update formulas differs only in the presence of additional weight decay term. The weight decay term limits the outputs weights in small values which improves model's generalization. This trait also underpins a compact and parsimonious network structure since an inactive hidden node can be deactivated by forcing its output weights to small values. The use of weight decay term adopts similar idea of generalized recursive least square (GRLS) method [43] but the GRLS method is designed under the global optimization framework where a global covariance matrix encompassing all hidden nodes is constructed. The global learning scenario is considered less feasible for online learning situation than the local approach since changing system structure calls for a resetting of output covariance matrix. Furthermore, the local learning scenario has been proven to be more robust against noise [14].
- **Stochastic Configuration Principle:** the theory of SCN has come into picture to resolve the underlying bottleneck in building randomized learners. The readers must be aware that the universal approximation property of randomized approaches do not always hold for the random parameters taken from the uniform distribution over the range of $[-1,1]$. It is worth mentioning that SCN starts its training process from scratch with no initial structure. The hidden node is incrementally constructed by virtue of the hidden node growing procedure. Details of the learning algorithms for building SCN can be read in [38] and it is omitted here for simplicity.

Since DSSCN works in the one-pass learning mode which prohibits to revisit preceding samples, the SC-II algorithm is implemented. That is, the

Table 2: Pseudocode of SCN-based Initialization Strategy

<p>Input: Data Chunk $(X, T) \in \mathbb{R}^{N \times (n+m)}$, the number of hidden nodes at the current time step R, the residual error $e_R(X) \in \mathbb{R}^{N \times m}$, the interval-valued activation degrees $\tilde{G}_{1:R}(X) \in \mathbb{R}^{N \times R}$ the user defined parameters: the maximum stochastic configuration T_{max}, a set of positive scalars $T = \{\lambda_{min}, \Delta\lambda, \lambda_{max}\}$ and $0 < r < 1$.</p>
<p>Output: Parameters of New Hidden Node $\sum_{R+1}^{-1} \in \mathbb{R}^{n \times n}$, $W \in \mathbb{R}^{R \times (2n+1) \times 1}$, $\Omega \in \mathbb{R}^{(2n+1) \times (2n+1)}$</p>
<p>IF A New Hidden Node is Added STEP 1: Allocate The Hidden Unit Parameters Using The SCN Concept - Inverse Covariance Matrix 1 Create two empty sets Φ, Ψ 2 For $\lambda \in T$ Do 3 For $k = 1, \dots, T_{max}$ Do 4 Randomly assign the input weight, the inverse covariance matrix in the range of $[-\lambda, \lambda]$ 5 Calculate the robustness variable $\zeta_{R+1,o}$ and $\mu_{R+1} = \frac{(1-r)}{(R+1)}$ 6 IF $\min(\zeta_{R+1,1}, \dots, \zeta_{R+1,m}) \geq 0$ 7 Save random parameters \sum_{R+1}^{-1} in the temporary matrix Ψ and $\zeta_{R+1} = \sum_{o=1}^m \zeta_{R+1,o}$ in Φ, respectively 8 End IF 9 End FOR 10 IF Ψ is not empty 11 Choose random parameters \sum_{R+1}^{-1}, maximizing ζ_{R+1} in Φ as parameters of new hidden node while the center of Gaussian unit as an incoming sample plus uncertainty factor $\underline{\mathcal{L}}_{R+1} = X_t - \delta, \overline{\mathcal{C}}_{R+1} = X_t + \delta$ 12 Break 13 Else randomly take $\tau \in (0, 1 - r)$, update $r = r + 1$ 14 End IF 15 End FOR Step 2: Allocate The Output Weight Parameters 18 Allocate the output weight vector and output covariance matrix of the new hidden node respectively as 19 $W_{R+1} = W_{win}, \Omega_{R+1} = \omega I$ END</p>

sliding window has to take at most as the size of data chunk and has to be completely discarded after being used. For simplicity, the size of sliding window is fixed as the size of data chunk. Table 2 outlines the pseudocode of SCN-based randomization strategy. The concept of SCN is applied when adding a new hidden node or when satisfying the hidden node growing condition determined using an extension of the recursive density estimation method [4]. It randomly select the inverse covariance matrix of the multivariate Gaussian function from a dynamic scope while the center of the multivariate Gaussian hidden node is set as an incoming data sample passing the hidden node growing condition. The output weight vector of a new hidden node is set as that of the winning node. The underlying reason is its closest proximity to the new hidden node, thus it is expected to characterize similar approximation curve. The output covariance matrix of the new hidden node in the FWGRLS method is assigned as $\Omega_{R+1} = \omega I$ where ω is a positive large constant. It is well-known that the convergence of FWGRLS method is assured when the new output covariance matrix is crafted as a large positive definite matrix. It is worth noting that the sliding window is applied to calculate the constraint parameter and the pseudo-inversion method is excluded from the learning procedure of eSCN. The parameter adjustment scenario is done using the FWGRLS method to expedite the training process.

5. Performance Evaluation

This section aims to numerically validate the efficacy of DSSCN by means of thorough simulations utilizing six synthetic and real-world data streams and comparisons with prominent data stream analytics methods in the literature. Simulations are undertaken under MATLAB environment of an Intel (R) Core i5-6600 CPU @ 3.3 GHZ with 8 GB of RAM and the MATLAB code of DSSCN is made publicly available in ¹ Three popular artificial data streams, namely SEA [34], SUSY [6] and Hyperplane [7], are used to test the performance of DSSCN, while DSSCN learning performance is also examined with two real-world data streams: electricity pricing valuation and weather prediction [8]. Another data stream problem is picked up from our indoor RFID localization problem in the manufacturing shopfloor where the underlying goal is to locate the position of raw materials in the production line [18]. DSSCN is also compared with data stream algorithms: pENsemble [30], Learn++.NSE [9], Learn++.CDS [8], pClass [24], eT2Class [29]. Moreover, the advantage of DSSCN is indicated by comparison with eSCN with the absence of deep stacked network architecture. The periodic hold-out process is followed as our simulation protocol [14]. That is, each data stream is divided into two parts where the first part is set for model updates, while the second part is exploited to assess the model’s generalization.

Table 3: SEA Dataset

Model	Classification Rate	Node	Layer/Local Model	Runtime	Input	Architecture
DSSCN	0.96±0.02	7.64±4.5	2.23±1.18	0.82±0.14	3	Deep
eSCN	0.95±0.02	1	1	0.46±0.27	3	Shallow
Learn++.NSE	0.93±0.02	N/A	200	1804.2	3	Ensemble
Learn++.CDS	0.93±0.02	N/A	200	2261.1	3	Ensemble
pENsemble	0.97±0.02	4.06±1.8	2.03±0.3	0.89±0.12	3	Ensemble
pClass	0.89±0.1	6.6±4.2	1	0.42±0.3	3	Shallow
eT2Class	0.88±0.23	1.5±0.5	1	0.34±0.11	3	Shallow

5.1. SEA Dataset

The SEA problem is a popular problem containing 100 K artificially generated data samples [34]. This problem is well-known for its abrupt drift component induced by three dramatic changes of the class boundary $\theta = 4 \rightarrow 7 \rightarrow 4 \rightarrow 7$. That is, this problem characterizes a binary classification problem where data samples are classified as the class 1 if it falls below the threshold $f_1 + f_2 < \theta$ while class 2 is returned if a sample is higher than the threshold $f_1 + f_2 > \theta$. Moreover, the modified version of Ditzler and Polikar is used in our numerical study where it differs itself from the original version in the class imbalanced and recurring drift properties with 5 to 25% minority class proportion. Data are drawn from the uniform distribution in the range of [0,10] and the prediction is underpinned by three input attributes but the third input attribute is

¹<http://www.deeps-cn.com/>

just a noise. Data stream environment is generated by batches of 1000 data samples with 200 time stamps and the concept drift takes place at every 50 time stamp. Figure 4(a)-(d) pictorially exhibits the trace of classification rate, hidden node, hidden layer and input weights. Table 3 tabulates consolidated numerical results of benchmarked algorithms.

The efficacy of DSSCN is evident in Table 3 where DSSCN delivers accurate prediction beating other algorithms except pENsemble. This result, however, should be carefully understood because of different base learners between DSSCN and pENsemble. pENsemble utilizes pClass as the base learner which fully learns all network parameters whereas eSCN is deployed in the DSSCN. That is, eSCN is designed following a randomized approach presenting rough estimation of the true solution. Figure 4(a) exhibits that DSSCN responds timely to concept drift where a new layer is introduced provided that a drift is identified. Furthermore, this fact also confirms that addition of new layer can be applied to cope with concept drift. A new layer characterizes recent observations and is placed at the top layer of deep stacked structure controlling the final output of the DSSCN. In addition, the layer merging mechanism functions to coalesce redundant layers, thereby relieving the model’s complexity. Adaptive feature weighting mechanism is exemplified in Figure 4(d) where an input feature showing high mutual information is assigned with a low weight to minimize its influence to the training process. Another interesting observation is found in the scope of random parameters. Hidden node parameters are randomly sampled from the range $[-0.5, 0.5]$, $[-1, 1]$, $[-2, 2]$ and $[-3, 3]$ automatically found in the training process. These ranges are fully data-driven where the SCN-based initialization strategy is executed whenever a new rule is created.

Table 4: Weather Dataset

Model	Classification Rate	Node	Layer/Local Model	Runtime	Input	Architecture
DSSCN	0.81±0.02	1.7±0.7	1.7±0.7	1.23±0.29	8	Deep
eSCN	0.69±0.03	15.5±3.4	1	6.51±2.29	8	Shallow
Learn++NSE	0.75±0.03	N/A	10	184.4	8	Ensemble
Learn++CDS	0.73±0.02	N/A	10	9.98	8	Ensemble
pENsemble	0.78±0.02	3±1.05	1.5±0.5	1.4±0.06	8	Ensemble
pClass	0.8±0.04	2.3±0.5	1	1.8±0.22	8	Shallow
eT2Class	0.8±0.03	2.3±0.3	1	1.8±0.1	8	Shallow

5.2. Weather Dataset

The weather dataset is exploited to examine the efficacy of DSSCN because it features recurring drift which uniquely refers to reappearance of previously seen data distribution due to seasonal changes. This dataset is a subset of NOAA database comprising daily weather data from different stations around the world. Among hundreds of weather stations, daily records of weather conditions from Offutt Air Force Base in Bellevue, Nebraska is chosen because it possesses the most complete recording for over 50 years which allows to portray

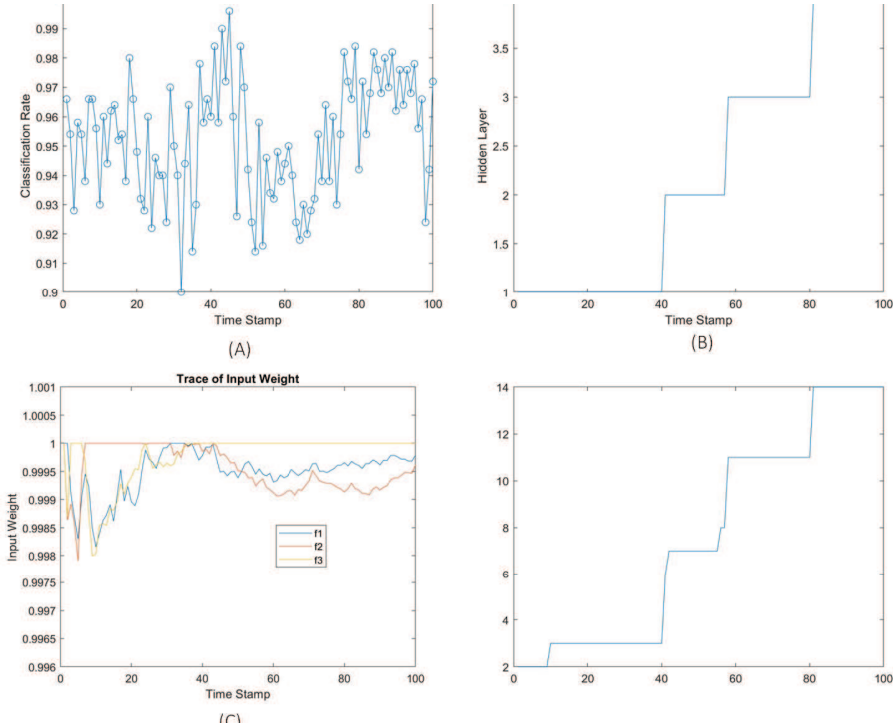


Figure 4: SEA data

not only ordinary seasonal change but also long-term climate change [8]. The underlying goal of this problem is to perform a binary classification of one-step-ahead weather prediction whether rain would occur on the next day with the use of eight input attributes. A total of 60000 data points are involved in our simulation where the average numerical results over ten time stamps are reported in Table 4. Figure 5 (a) exhibits the evolution of DSSCN classification rates and Figure 5(b) depicts the evolution of hidden nodes, while the evolution of hidden layer is shown in Figure 5(c) and the trace of input weights is visualized in Figure 5(d).

Referring to Table 4, DSSCN outperforms other benchmarked algorithms in terms of predictive accuracy and hidden layers/local experts. It is observed that DSSCN indicates significant performance improvement over eSCN using a shallow network structure. Compared to pENsemble - an evolving ensemble learner, DSSCN produces slightly more inferior predictive accuracy than pENsemble but involves lower number of local experts. DSSCN also undergoes the fastest training speed than other algorithms. This fact can be explained from the update strategy of DSSCN where only the top hidden layer is subject to the tuning phase. In addition, eSCN encompasses all data samples of the data chunk during construction of new base building unit to discover the best scope of hidden node parameters. Figure 5(b) and 5(c) confirms the growing

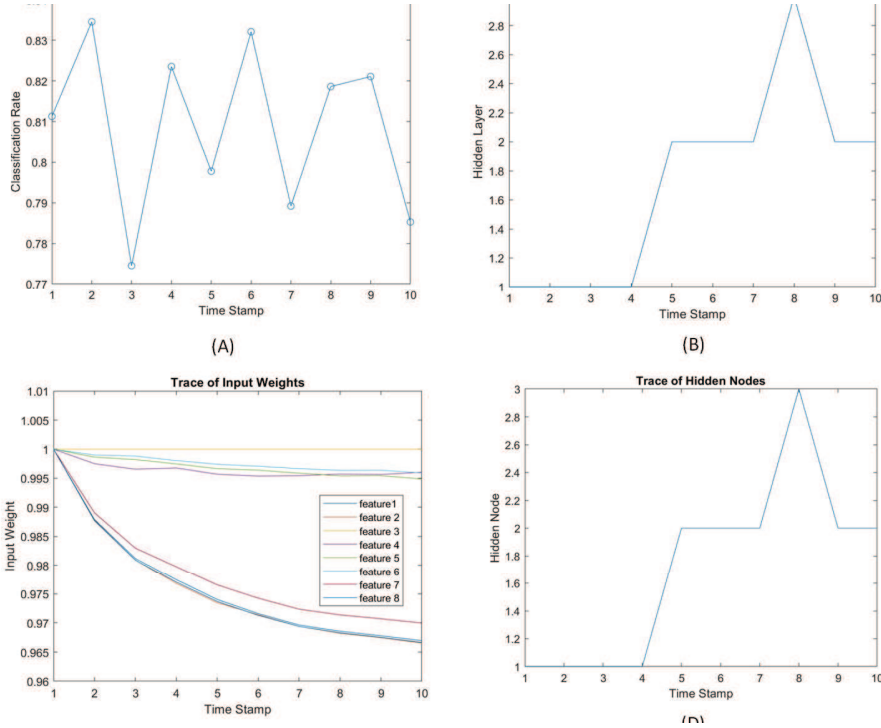


Figure 5: weather data

and pruning property of DSSCN in which it is not only capable of self-organizing its hidden nodes but also its hidden layers with addition and removal of base building units. As portrayed in Fig. 5(d), the online feature weighting mechanism controls the influence of input features where it allows an input feature to pick up again in the future. The SCN-based initialization strategy produces the scope of $[-100,100]$ applied to generate new hidden node parameters. It is worth mentioning that the SCN-based initialization strategy is executed in the main training process of eSCN.

Table 5: Electricity Pricing Dataset

Model	Classification Rate	Node	Layer/Local Model	Runtime	Input	Architecture
DSSCN	0.74±0.15	4.96±3.08	1.4±0.49	0.2±0.07	4	Deep
eSCN	0.73±0.17	1	1	0.04±0.006	4	Shallow
Learn++NSE	0.69±0.08	N/A	119	211.2	4	Ensemble
Learn++CDS	0.69±0.08	N/A	119	211.2	4	Ensemble
pENsemble	0.75±0.16	1.01±0.07	1.01±0.07	1.4±0.06	4	Ensemble
pClass	0.68±0.1	3.5±2.4	1	7.1±4.4	4	Shallow
eT2Class	0.72±0.17	4.6±1.3	1	0.3±0.08	4	Shallow

5.3. Electricity Pricing Dataset

The electricity pricing dataset describes prediction of electricity demand fluctuation in the state of New South Wales (NSW), Australia where the main objective is to forecast whether the electricity price of NSW in the next 24 hours will be higher than that of Victoria. Four input attributes, namely the day, period, NSW electricity demand and Victorian electricity demand, and the scheduled electricity transfer, are put forward to guide the electricity demand prediction. Furthermore, the modified electricity pricing dataset in [8] is used to simulate the class imbalance problem with the imbalance ratio of 1:18 by performing undersampling to the minority class. It is worth mentioning that this problem features the non-stationary characteristic as a result of dynamic market condition and economic activities. Numerical results of all consolidated algorithms are reported in Table 5.

DSSCN clearly delivers promising performance where it is only inferior to pENsemble in terms of accuracy by about 1 %. Compared to its shallow counterpart, eSCN, the use of a deep network structure is capable of delivering improvement of model’s generalization. The unique trait of DSSCN is viewed in the incremental construction of deep network structure where not only hidden nodes can be automatically grown and pruned but also hidden layer is fully self-organized. This elastic structure adapts to concept drifts because concept drift can be identified and reacted in accordance with its severity and rate. The adaptive scope selection property of DSSCN is substantiated by the fact that [-3,3] is selected during the training process.

Table 6: Susy Dataset

Model	Classification Rate	Node	Layer/Local Model	Runtime	Input	Architecture
DSSCN	0.78±0.03	10.37±3.4	10.37±3.4	0.34±0.03	4	Deep
eSCN	0.76±0.04	18.9±11.92	1	18.3±20.08	4	Shallow
pENsemble	0.76±0.04	1.6±0.7	2.84±1.4	0.6±0.28	4	Ensemble
pClass	0.73±0.06	1.96±0.26	1	0.79±0.3	4	Shallow
eT2Class	0.74±0.06	5.2±1.5	1	2.42±0.6	4	Shallow

5.4. Susy Dataset

Susy problem actualizes a big streaming data problem consisting of five millions records allowing algorithmic validation in the lifelong learning fashion. This problem is a binary classification problem produced by Monte Carlo simulations and describes classification of signal process that generates super-symmetric particles [6]. The classification problem is guided with the use of 18 input attributes where the first eight input attributes present the kinematic properties while the remainders are simply the function of the first eight input features. All benchmarked algorithms are run through 10000 data batches where each batch carries 500 data samples. 400 data points are reserved for model updates while the rest of 100 samples are exploited for validation. The training samples are collected from the first 4.5 millions of data samples while the testing data are sampled from the next 500 K data points. Numerical results

of consolidated algorithms are summarized in Table 6. Figure 6(a) visualizes the trace of classification rates and Figure 6(b) exhibits the trace of hidden nodes, while the trace of hidden layers and feature weights are displayed in Figure 6(c) and Figure 6(d) respectively.

From Table 6, DSSCN delivers the highest classification rate. It is shown that DSSCN’s deep hierarchical network and learning modules has led to 2% improvement of predictive accuracy of eSCN relying on a shallow network architecture. DSSCN also outperforms other benchmarked algorithms in term of execution time. This fact differs from the ensemble learner where one can simply adjust the most relevant ensemble member because each of them is loosely coupled. Figure 6(b) also depicts the incremental construction of deep neural network where new layer can be incorporated on demand while redundant layers can be merged. It is observed that DSSCN actualizes dynamic confidence levels of drift detector where initially the confidence level is set high but gradually reduces by means of the exponentially decaying function (18). This setting makes possible to increase the depth of neural network more intensively as more training samples become available. It is well-known that the success of deep neural network is subject to sample’s availability whereas a shallow neural network is preferred for a small dataset. Because the drift detection method is applied to grow the network structure, the decrease of confidence level is capped at 90% to prevent introduction of hidden layers during the drift-free state. Learn++NSE and Learn++CDS are excluded from this problem because they were terminated before obtaining numerical results although they have been executed for three days. the scope of $[-100,100]$ is automatically picked up by the SCN-based initialization strategy in this numerical example.

Table 7: Hyperplane Dataset

Model	Classification Rate	Node	Layer/Local Model	Runtime	Input	Architecture
DSSCN	0.92±0.02	9.3±1.98	1.89±0.37	0.54±0.13	2	Deep
eSCN	0.92±0.02	4.21±0.54	1	0.82±0.15	2	Shallow
Learn++NSE	0.91±0.02	N/A	100	926.04	2	Ensemble
Learn++CDS	0.9±0.0	N/A	100	2125.5	2	Ensemble
pENsemble	0.92±0.02	2.7±0.7	1.87±0.34	0.7±0.23	2	Ensemble
pClass	0.91±0.02	3.8±1.7	1	2.7±1.4	2	Shallow
eT2Class	0.89±0.1	2.04±0.2	1	2.5±1.5	2	Shallow

5.5. Hyperplane Dataset

The hyperplane problem presents a binary classification problem classifying a d-dimensional data point into two classes with respect to the position of a random hyperplane. This problem is taken from the Massive Online Analysis (MOA) [7] - an open source software for data stream analytics. The prominent characteristic of this problem is found in the gradual drift where initially data samples are drawn from a single data distribution with probability one. The

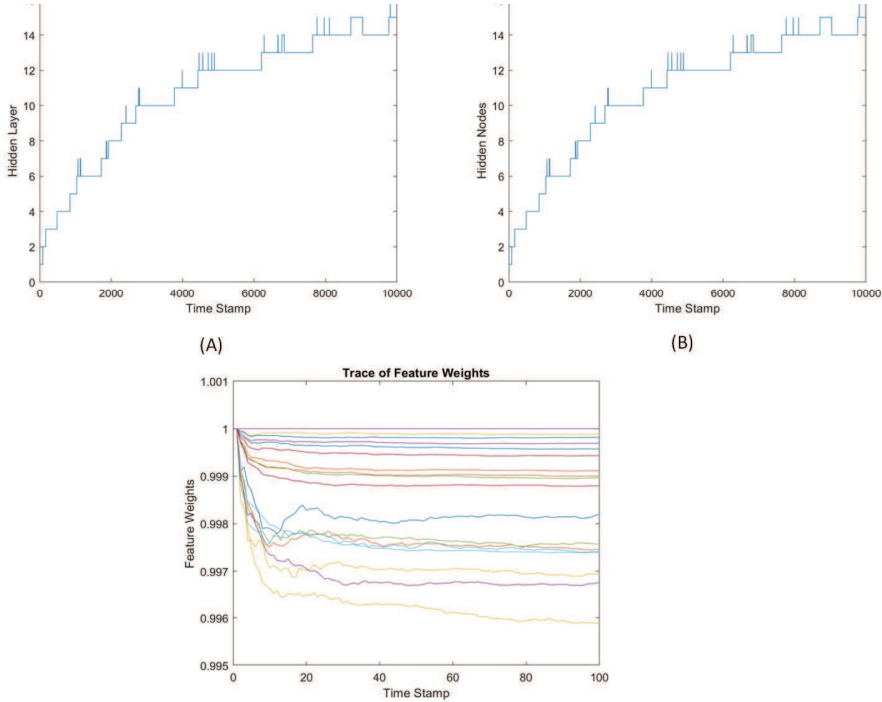


Figure 6: SUSY data

transition period takes place by the introduction of the second distribution which slowly interferes data generation process before completely replaces the first data distribution. A data sample is assigned as class 1 if $\sum_{i=1}^d x_i w_i > w_0$ is satisfied whereas class 2 is returned if the condition is violated. This dataset carries 120 K samples equally partitioned into 100 data batches without changing data order to simulate data stream environments. Each data stream comprises 1200 samples where the first 1000 samples are injected for the training process while the rest is reserved for testing samples. The concept drift comes into picture after the 40th time stamp. Table 7 sums up numerical results of all consolidated algorithms.

DSSCN delivers the most encouraging performance in terms of accuracy and network complexity. Compared to Learn++ family, DSSCN offers more parsimonious network structure because a new data stream does not necessarily cause addition of a new local expert due to the use of drift detection mechanism. It is also observed that DSSCN's runtime is comparable to that shallow neural network variants because only the top layer is fine-tuned. It is also reported that the scope of random parameters are obtained from the ranges of $[-1,1], [-1.5,1.5], [-2,2], [-3,3]$ confirming the adaptive scope selection of DSSCN.

Table 8: RFID Dataset

Model	Classification Rate	Node	Layer/Local Model	Runtime	Input	Architecture
DSSCN	0.99±0.02	5.2±0.56	1.04±0.2	1.97±0.46	1	Deep
eSCN	0.92±0.08	18.69±11.92	1	18.3±20.08	1	Shallow
Learn++NSE	0.99±0.01	N/A	100	5.69±56.88	1	Ensemble
Learn++CDS	0.99±0.01	N/A	100	7.99±9.92	1	Ensemble
pENsemble	0.67±0.02	2.02±0.2	1.01±0.07	0.89±0.12	1	Ensemble
pClass	0.95±0.08	2	1	1.13±0.25	1	Shallow
eT2Class	0.94±0.04	2	1	1.13±0.24	1	Shallow

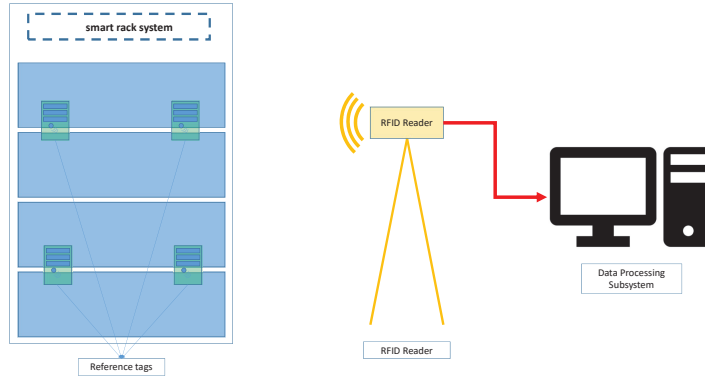


Figure 7: RFID localization testbed

5.6. RFID Dataset

RFID-based localization has gained increasing popularity and is capable of achieving millimetre accuracy [18]. Furthermore, the use of COTS readers feeding the phase information of the RF backscatter signal from the RFID signal enhances object tracking accuracy. This approach offers a cheaper solution than traditional approach in the object localization involving deployment of antennas for every single object on a rack. This problem presents the RFID-based localization in the manufacturing shopfloor where the main goal is to track objects placed on the rack or shells based on the phase information of the RFID tags (Courtesy of Dr. Huang Sheng, Singapore). The application of machine learning for the RFID based localization allows improvement of RFID-based localization because the phase signal is heavily affected by the positional changes of the objects. In addition, multiple items on the rack influences the signal phase and amplitude distribution of a target tag. Online learning is highly demanded in this application to solve the so-called multipath effect due to reflections and scattering distorting the RSSI and phase of the signal. This problem is frequently encountered positional configurations of the rack or shells or the sudden presence of unknown objects. Figure 7 illustrates our test bed.

The test bed consists of a steel storage rack with five compartments where each compartment is occupied by 5-6 objects with different dimensions attached with COTS RFID tags. Two UHF antennas are mounted on the rack and

Table 9: Scopes of Random Parameters

Problems	Ranges
SEA	$[-0.5, 0.5], [-1, 1], [-2, 2], [-3, 3]$
Weather	$[-100, 100]$
Electricity	$[-3, 3]$
SUSY	$[-100, 100]$
Hyperplane	$[-1, 1], [-1.5, 1.5], [-2.2], [-3, 3]$
RFID	$[-0.1, 0.1], [-1, 1], [-2, 2], [-3, 3]$

connected to COTS RFID receiver. The RSSI and phase signals reading of the COTS RFID receiver will be transmitted to the host computer by means of Ethernet connections. The rack is divided into four zones by the installment of four RFID reference tags in different sections of the rack. The RFID dataset contains 281.3 K records of RSSI and phase signals with four target classes corresponding to the four zones of the rack. Our experiment is carried out using the periodic hold out protocol with 100 time stamps. In each time stamp, 2 K data samples are exploited for model updates, while the rest 813 data points are fed to examine model’s generalization potential. Consolidated numerical results are summed up in Table 8.

DSSCN produces promising generalization power attaining 99% classification rate. It is comparable to Learn++NSE and Learn++CDS but incurs less complexity in terms of training speed and network complexities because DSSCN realizes controlled growth of network structure where a new data stream does not necessarily triggers addition of new building units. The importance of the network depth is borne out in Table 13 where it delivers 7% improvement on accuracies compared to its shallow counterpart, eSCN. It is also shown that eSCN runtime is more sluggish than those eT2Class and pClass because it has to fully utilize all samples in the data chunk to execute the scope selection procedure. It is worth noting that the sliding window size in our numerical study is fixed as the data chunk size. $[-0.1, 0.1], [-1, 1], [-2, 2], [-3, 3]$ are selected by the SCN-based initialization strategy. Note that SCN-based initialization strategy is triggered on the fly whenever a new hidden node is appended. In other words, every hidden node are randomly crafted from dynamic random sampling scopes. Table 9 displays the ranges of random parameter produced by the SCN-based initialization strategy.

6. Conclusions

The salient property of the proposed DSSCN is indicated by its open structure principle which allows automated construction of deep neural network from scratch on the fly. The network structure of DSSCN can be automatically generated by incrementally inserting new hidden layers and/or new hidden nodes while implementing the network complexity reduction mechanism using the hidden layer merging mechanism and the hidden node pruning mechanism. Fur-

thermore, all learning modules of DSSCN work fully online in the chunk by chunk basis where data chunk is discarded once learned without revisiting them again in the future. DSSCN is built upon evolving stochastic configuration networks (eSCNs) which embraces recently developed stochastic configuration networks (SCNs). The SCN framework incorporates the constraint of random parameters forming the adaptive scope selection which adapts to the real data distribution. Moreover, eSCN realizes a self-organizing property where hidden nodes can be automatically added and pruned on the fly. This trait enhances the adaptive nature of deep neural network and is capable of handling local drift better than a static base building unit. The deep network structure is developed using the stacked generalization principle where each base building unit or hidden layer is seriesly connected in tandem. That is, each base building unit receives the original input vector plus the random shift driven by the output of preceding layer.

The self-organizing property of DSSCN is governed by a drift detection method where a network structure is deepened by addition of a new hidden layer if a concept drift is detected. The drift threshold is determined from the Hoeffding’s bound concept with exponentially decaying confidence level providing clear link between rate of growth of network structure and sample availability. The network complexity reduction scenario relies on a network merging scenario which analyses mutual information of each base building unit. Moreover, DSSCN is equipped by the online feature weighting mechanisms by virtue of feature redundancy where an input feature having high mutual information with other input attributes is assigned with a low input effect to rule out its influence to the overall training process.

The advantages of DSSCN has been validated using six real-world and synthetic datasets featuring non-stationary characteristic. Furthermore, DSSCN has been numerically validated in our real-world project, namely RFID-based localization in the manufacturing shopfloor. Compared to five prominent algorithms for data streams, our proposed DSSCN demonstrates state-of-the art performance. It is worth noting that eSCN has no tuning mechanism of hidden nodes rather random parameters are sampled from adaptively selected scope. Although the random parameter constraint imposes the use of all data points in the data chunk during the creation of new base building unit which slows down model updates, numerical results shows that a comparable training speed can be achieved. This result is mainly caused by the update strategy of DSSCN where only the top layer is fine-tuned during the stable condition to generate different input representations. In addition, this update strategy is confirmed by the relevance of the top layer because it is supposed to represent the closest concept to the original data distribution. That is, it is added when the latest concept change is signalled.

Although the drift detection mechanism has been demonstrated to be very effective in growing the depth of deep neural networks, it does not evaluate model’s generalization. It is well-known that the depth of deep neural networks has direct influence to the generalization power. Our future work will be focused on the algorithmic development of generalization-based criteria to evolve the

structure of deep neural networks. Also, we will investigate the application of proposed methodologies to other deep learning variants including CNN and LSTM in our future studies.

7. Acknowledgement

This work is fully supported by Ministry of Education, Republic of Singapore, Tier 1 Research Grant and NTU Start-up Grant. The authors also thank Singapore Institute of Manufacturing Technology (SIMTech), Singapore for providing RFID dataset and acknowledge the assistance of Mr. MD. Mef-tahul Ferdaus for Latex typesetting of this paper.

8. References

References

- [1] R. H. Abiyev and O. Kaynak. Type 2 fuzzy neural structure for identification and control of time-varying plants. *IEEE Transactions on Industrial Electronics*, 57(12):4147–4159, 2010.
- [2] M. Alhamdoosh and D. Wang. Fast decorrelated neural network ensembles with random weights. *Information Sciences*, 264:104–117, 2014.
- [3] P. Angelov. *Autonomous learning systems: from data streams to knowledge in real-time*. John Wiley & Sons, 2012.
- [4] P. Angelov and D. P. Filev. An approach to online identification of takagi-sugeno fuzzy models. *IEEE Transactions on Systems, Man, and Cybernetics, Part B (Cybernetics)*, 34(1):484–498, 2004.
- [5] P. Angelov and R. Yager. A new type of simplified fuzzy rule-based system. *International Journal of General Systems*, 41(2):163–185, 2012.
- [6] P. Baldi, P. D. Sadowski, and D. Whiteson. Searching for exotic particles in high-energy physics with deep learning. *Nature communications*, 5:4308, 2014.
- [7] A. Bifet, G. Holmes, R. Kirkby, and B. Pfahringer. Moa: Massive online analysis. *J. Mach. Learn. Res.*, 11:1601–1604, August 2010.
- [8] G. Ditzler and R. Polikar. Incremental learning of concept drift from streaming imbalanced data. *IEEE Transactions on Knowledge and Data Engineering*, 25(10):2283–2301, October 2013.
- [9] R. Elwell and R. Polikar. Incremental learning of concept drift in nonstationary environments. *IEEE Transactions Neural Networks*, 22(10):1517–1531, October 2011.

- [10] I. Frias-Blanco, J. d. Campo-Avila, G. Ramos-Jimenez, R. Morales-Bueno, A. Ortiz-Diaz, and Y. Caballero-Mota. Online and non-parametric drift detection methods based on hoeffdings bounds. *IEEE Transactions on Knowledge and Data Engineering*, 27(3):810–823, March 2015.
- [11] B. Igelnik and Y-H. Pao. Stochastic choice of basis functions in adaptive function approximation and the functional-link net. *IEEE Transactions on Neural Networks*, 6(6):1320–1329, 1995.
- [12] A. Krizhevsky, I. Sutskever, and G. Hinton. Imagenet classification with deep convolutional neural networks. In F. Pereira, C. J. C. Burges, L. Bottou, and K. Q. Weinberger, editors, *Advances in Neural Information Processing Systems 25*, pages 1097–1105. Curran Associates, Inc., 2012.
- [13] M. Li and D. Wang. Insights into randomized algorithms for neural networks: Practical issues and common pitfalls. *Information Sciences*, 382–383:170–178, 2017.
- [14] E. Lughofer. *Evolving Fuzzy Systems-Methodologies, Advanced Concepts and Applications*, volume 53. Springer, 2011.
- [15] E. Lughofer, C. Cernuda, S. Kindermann, and M. Pratama. Generalized smart evolving fuzzy systems. *Evolving Systems*, 6(4):269–292, 2015.
- [16] Jerry M. Mendel. General type-2 fuzzy logic systems made simple: A tutorial. *IEEE Transactions on Fuzzy Systems*, 22:1162–1182, 2014.
- [17] P. Mitra, C. A. Murthy, and S. K. Pal. Unsupervised feature selection using feature similarity. *IEEE Transactions on Pattern Analysis and Machine Intelligence*, 24(3):301–312, 2002.
- [18] M. V. Moreno-Cano, M. A. Zamora-Izquierdo, José Santa, and Antonio F. Skarmeta. An indoor localization system based on artificial neural networks and particle filters applied to intelligent buildings. *Neurocomputing*, 122:116–125, December 2013.
- [19] Y-H. Pao, G-H. Park, and D. J. Sobajic. Learning and generalization characteristics of the random vector functional-link net. *Neurocomputing*, 6(2):163–180, 1994.
- [20] Y-H. Pao and Y. Takefuji. Functional-link net computing: Theory, system architecture, and functionalities, special issue of computer on computer architectures for intelligent machines. *IEEE Computer Society Press*, 3:76–79, 1991.
- [21] Y-H. Pao and Y. Takefuji. Functional-link net computing: theory, system architecture, and functionalities. *Computer*, 25(5):76–79, 1992.

- [22] J. C. Patra and A. C. Kot. Nonlinear dynamic system identification using chebyshev functional link artificial neural networks. *IEEE Transactions on Systems, Man, and Cybernetics, Part B (Cybernetics)*, 32(4):505–511, 2002.
- [23] M. Pratama, S. G. Anavatti, P. Angelov, and E. Lughofer. PANFIS: a novel incremental learning machine. *IEEE Transactions on Neural Networks and Learning Systems*, 25(1):55–68, 2014.
- [24] M. Pratama, S. G. Anavatti, M-J. Er, and E. D. Lughofer. pClass: an effective classifier for streaming examples. *IEEE Transactions on Fuzzy Systems*, 23(2):369–386, 2015.
- [25] M. Pratama, S. G. Anavatti, and J. Lu. Recurrent classifier based on an incremental metacognitive-based scaffolding algorithm. *IEEE Transactions on Fuzzy Systems*, 23(6):2048–2066, 2015.
- [26] M. Pratama, S. G. Anavatti, and E. Lughofer. Genefis: toward an effective localist network. *IEEE Transactions on Fuzzy Systems*, 22(3):547–562, 2014.
- [27] M. Pratama, P. P. Angelov, E. Lughofer, and M-J Er. Parsimonious random vector functional link network for data streams. *Information Sciences*, 430-431:519 – 537, 2018.
- [28] M. Pratama, J. Lu, E. Lughofer, G. Zhang, and S. Anavatti. Scaffolding type-2 classifier for incremental learning under concept drifts. *Neurocomputing*, 191:304–329, 2016.
- [29] M. Pratama, J. Lu, and G. Zhang. Evolving type-2 fuzzy classifier. *IEEE Transactions on Fuzzy Systems*, 24(3):574–589, 2016.
- [30] M. Pratama, W. Pedrycz, and E. Lughofer. Evolving ensemble fuzzy classifier. *IEEE Transactions on Fuzzy Systems*, pages 1–1, 2018.
- [31] D. Sahoo, Q. D. Pham, J. Lu, and S. C. Hoi. Online deep learning: Learning deep neural networks on the fly. *arXiv preprint arXiv:1711.03705*, abs/1711.03705, 2017.
- [32] W. F. Schmidt, M. A. Kraaijveld, and R. PW Duin. Feedforward neural networks with random weights. In *Pattern Recognition, 1992. Vol. II. Conference B: Pattern Recognition Methodology and Systems, Proceedings., 11th IAPR International Conference on*, pages 1–4. IEEE, 1992.
- [33] H. B. Sola, J. Fernandez, H. Hagrais, F. Herrera, M. Pagola, and E. Barrenechea. Interval type-2 fuzzy sets are generalization of interval-valued fuzzy sets: Toward a wider view on their relationship. *IEEE Transactions on Fuzzy Systems*, 23(5):1876–1882, Oct 2015.

- [34] W. N. Street and Y-S Kim. A streaming ensemble algorithm (sea) for large-scale classification. In *Proceedings of the Seventh ACM SIGKDD International Conference on Knowledge Discovery and Data Mining*, KDD '01, pages 377–382, New York, NY, USA, 2001. ACM.
- [35] D. Wang and C. Cui. Stochastic configuration networks ensemble with heterogeneous features for large-scale data analytics. *Information Sciences*, 417(10):55–71, 2017.
- [36] D. Wang and M. Li. Deep stochastic configuration networks with universal approximation property. *arXiv preprint arXiv:1702.05639 and also presented at 2018 International Joint Conference on Neural Networks*, 2017.
- [37] D. Wang and M. Li. Robust stochastic configuration networks with kernel density estimation for uncertain data regression. *Information Sciences*, 417(10):210–222, 2017.
- [38] D. Wang and M. Li. Stochastic configuration networks: Fundamentals and algorithms. *IEEE transactions on cybernetics*, 47(10):3466–3479, 2017.
- [39] J. Wang, P. Zhao, S. CH. Hoi, and R. Jin. Online feature selection and its applications. *IEEE Transactions on Knowledge and Data Engineering*, 26(3):698–710, 2014.
- [40] L. Wang, H-B. Ji, and Y. Jin. Fuzzy passive-aggressive classification: A robust and efficient algorithm for online classification problems. *Information Sciences*, 220:46–63, January 2013.
- [41] D. H. Wolpert. Stacked generalization. *Neural Networks*, 5(2):241–259, 1992.
- [42] D. H. Wolpert. The power of depth for feed-forward neural networks. *Journal of Machine Learning Research*, 49:1–39, 2016.
- [43] Y. Xu, K-W. Wong, and C-S. Leung. Generalized RLS approach to the training of neural networks. *IEEE Transactions on Neural Networks*, 17(1):19–34, 2006.
- [44] J. Yoon, E. Yang, and S-J. Hwang. Lifelong learning with dynamically expandable networks. *arXiv preprint arXiv:1708.01547*, 2017.
- [45] C. Yu, F. X. Yu, R. S. Feris, S. Kumar, A. N. Choudhary, and S-F. Chang. An exploration of parameter redundancy in deep networks with circulant projections. *International Conference on Computer Vision (ICCV)*, pages 2857–2865, 2015.
- [46] C. Zain, M. Pratama, M. Prasad, C-P. Lim, and M. Seera. Motor fault detection and diagnosis based on evolving random vector functional link network. *Diagnostic and Prognostic of Hybrid Systems*, 2018.

- [47] Y. Zhang, H. Ishibuchi, and S. Wang. Deep takagi-sugeno-kang fuzzy classifier with shared linguistic fuzzy rules. *IEEE Transactions on Fuzzy Systems*, 26(3):1–1, 2017.
- [48] T. Zhou, F-L. Chung, and S. Wang. Deep TSK fuzzy classifier with stacked generalization and triplely concise interpretability guarantee for large data. *IEEE Transactions on Fuzzy Systems*, 25(5):1207–1221, 2017.